



## Research article

# Ultrafiltration membrane based on chitosan/adipic acid: Synthesis, characterization and performance on separation of methylene blue and reactive yellow-145 from aqueous phase

Khaled Hab Alrman<sup>\*</sup>, Sahar Alhariri, Iman Al- Bakri*Department of Chemistry, Faculty of Science, Damascus University, Syrian Arab Republic*

## ARTICLE INFO

**Keywords:**

Chitosan- adipic acid- cross-linking- separation- organic dyes

## ABSTRACT

Here, we report for the first time using of the nontoxic chitosan/adipic acid cross-linked membrane CS/AA in the separation of methylene blue and reactive yellow-145 from aqueous phase. The reason we chose adipic acid as a cross-linking agent is because it gives the cross-linked membrane moderate flexibility due to the presence of four methylene groups in its structure. The structure of the cross-linked membrane CS/AA and their properties were confirmed through, FTIR, differential scanning calorimetry (DSC), thermogravimetric analysis (TGA), atomic force microscopy (AFM), and BET analysis. The thermal properties of membrane indicated an improvement in its flexibility and hydrophobicity, but this improvement was accompanied by a decrease in its thermal stability.  $pH_{pzc}$  value and porosity of the CS/AA were 7.88, and 73.95 % respectively. The average pore radius distribution ranged from 2 to 27 nm. The prepared cross-linked membrane provides spontaneous and continuous purification of water with a high efficiency. This is due to the membrane CS/AA ability to separate methylene blue and reactive yellow-145 from the aqueous phase almost completely. The results revealed that the removal efficiency and permeation flux for MB were 100 % and 1 L/m<sup>2</sup>.h respectively at initial dye concentration of (4,8) mg/L, at 1 bar, and the removal efficiency and permeation flux for RY-145 were (94,96) % and (1.06, 2.09) L/m<sup>2</sup>.h respectively at 100 mg/L and at (1,1.5) bar. Such cross-linked nanopore polymer membranes provide a new approach for emerging novel purification systems, principally in the field of environmental field.

## 1. Introduction

Dyes are one of the main water pollutants, that are used in various fields, especially textile industries [1]. These compounds exist in aqueous phases in cationic or anionic structure [2]. Many dyes found in polluted water are non-biodegradable, toxic, and carcinogenic. Therefore, it has harmful effects on public health and causing serious environmental concerns [3]. Additionally, it is difficult to remove dyes from water bodies due to their high solubility in water and chemical stability [4]. Therefore, it is important to use an effective method to remove these pollutants. To solve this problem, various water treatment techniques have been developed, including chemical precipitation, solvent extraction, electrocoagulation, advanced oxidation processes, adsorption, and membrane filtration [5, 6]. In recent years, membrane technology has developed significantly due to its high effectiveness in removing contaminants from the

<sup>\*</sup> Corresponding author.

E-mail address: [khaled.alruman@damascusuniversity.edu.sy](mailto:khaled.alruman@damascusuniversity.edu.sy) (K. Hab Alrman).

aqueous phase in order to obtain pure water. Membrane technology has many properties such as low economic cost, high efficiency, no need for complex equipment, environmental respect and ease of use. This means that membrane technology is one of the suitable solutions for wastewater treatment [7]. Due to its multidisciplinary nature, membrane technology is used in a number of industries, including domestic and industrial water treatment, desalination [8], removal of organic compounds [9], chemical processes, pharmaceuticals, metallurgy and other separation processes [10] such as separation of gas mixtures [11], or capture of CO<sub>2</sub> from the atmosphere [12]. Membranes suffer from many problems wetting, fouling, and flux decline phenomena [13], so there is a clear trend in creating outperforming membranes. Ultrafiltration is one of the technologies used in various fields, such as chemical, electronic, food, and biotechnical industries, especially recovery of chemical compounds, water treatment, juice concentration, and drinking water purification [14]. UF technology is characterized by high effectiveness in removing organic and inorganic pollutants from aqueous phases, in addition to low energy consumption and non-existent chemical use, which makes it superior to traditional treatment methods [15,16]. Chitosan is a natural polymer, which is the most abundant natural polysaccharide on earth after the cellulose in terms of its availability [17,18]. The chitosan, obtained from the deacetylation of chitin either by enzymatic or chemical method, has several properties such as biocompatibility, nontoxicity, and biodegradability [17,19]. Therefore, chitosan is a lot advantageous for the water purification from numerous pollutants such removal of dyes, phenols, heavy metal ions and pesticides [20], because its structure contains hydroxyl and amine groups [21]. However, there are considerable limitations, such as poor acid stability, limited surface area, low mechanical strength and chemical resistance [22]. To overcome the previous limitations, modifications can be achieved to the amine or hydroxyl groups present in the polymer chain through grafting or cross-linking processes [23,24]. Amino groups are highly reactive under acidic conditions, so the order of reactivity under acidic conditions is usually: NH<sub>2</sub> > -OH<sub>(primary)</sub> > -OH<sub>(secondary)</sub>, whereas in alkaline medium the reactivity of primary hydroxyl group of chitosan is greater than the reactivity of amino group [25]. Cross-linking processes are commonly used to improve the physicochemical and mechanical properties of chitosan-based materials [23,26,27]. There are many cross-linking agents for chitosan such as genipin, glutaraldehyde, diglycidyl ether, triphosphosphate, diisocyanate and dicarboxylic acids [28]. Adipic acid is used in various fields, especially in the food industry, as an acidifier, gelling aid. This acid has two carboxyl groups [29]. Therefore, it can be used as a safe solvent and cross-linking agent for chitosan [30,31]. Some investigations have been conducted to modify chitosan using cross-linking agent. For instance, Raza and his coworkers synthesized cross-linked membrane based on (chitosan/polyethylene glycol-300) and tetraethyl orthosilicate as a cross-linker. The permeation results revealed that NaCl rejection and flux of the modified membranes increased up 60 % and 86.36 mL/h.m<sup>2</sup>, respectively [32]. While Israr Ali. et al. synthesized cross-linked nanofibrous based on (chitosan/polyvinylpyrrolidone) and maleic acid as cross-linkers at different concentrations. The active layer was electrospun on a 3-triethoxysilylpropylamine functionalized cellulose acetate substrate. The performance of the prepared membranes was evaluated by changing the concentration of the cross-linking agent from 0.5 % to 2.5 % w/v. The best rejection and flux value of NaCl (3.28 wt%) at 55.2 bar were 98.3 % and 42.9 L/m<sup>2</sup>.h, respectively [33]. In another work, Chen, A. et al. synthesized cross-linking adsorbent material based on (chitosan/epichlorohydrin) to remove (Zn<sup>2+</sup>, Cu<sup>2+</sup> and Pb<sup>2+</sup>) ions from aqueous phase. The adsorption and Kinetics study was carried out. It was found that the adsorption of the three ions is monolayer coverage through physical adsorption phenomena [34]. In another study, Sosa, J. M. et al. prepared a cross-linking membrane based on (chitosan/Graphene Oxide). The (CS/GO) cross-linked membrane's performance was tested using cross-flow unit to remove methylene blue dye at concentrations (1–100) mg/L at p = 345 kPa. The permeation flux and removal were ranged (1–4.5) L/m<sup>2</sup>.h and 100 % respectively [35]. The primary purpose of this work was to use the cross-linked membrane CS/AA in the separation of organic dyes from wastewater and to investigate the factors that effect on the cross-linked membrane performance, including concentration, pressure, and stages of continuous separation using a dead-end filtration system. The mechanism by which the membrane removes the contaminant was also explained. In order to perform the detailed characterization of prepared membranes, commonly available methods were applied such as FTIR, DSC, TGA, DTG, BET, AFM and pH<sub>pzc</sub>. In addition to, the physical and mechanical properties and chemical stability were determined.

## 2. Materials and methods

### 2.1. Materials

Chitosan Powder (CS) (DDA = 95 %, M<sub>w</sub> = 200 kDa) was purchased from Golden-Shell Biochemical Co.ltd), glacial acetic acid was purchased from Paneeac, sodium hydroxide from Scp Surechem Products, adipic acid was purchased from Riedel-de Haën, hydrochloric acid from Paneeac, methylene blue was provided by Merck, reactive yellow-145 was supplied from Oh Young Industry, ethanol was purchased from Sham lab, sodium chloride was purchased from Fisher chemical, n-Hexane was purchased from Scp Surechem. All solutions were prepared with distilled water.

### 2.2. Preparation of membranes

The pure chitosan (CS) membrane was prepared using the casting method described elsewhere [36]. The chitosan powder 1.5 g (8.8 mmol) was dissolved in 100 mL of 0.1 M acetic acid solution then the solution was agitated for 24 h at room temperature and sonicated with an ultrasonic 206 (rocker, 50 Hz) to remove bubbles. The polymer solution was then poured onto a polypropylene dish (surface area = 25.18 cm<sup>2</sup>) as a thin membrane. The solvent was evaporated at a temperature of 30 °C until the membrane dried and separated from the dish. The membrane was then immersed in 0.1 M NaOH, rinsed with distilled water until neutral, and dried at 70 °C. Finally, the thickness of the membrane was measured using a digital thickness gauge, and its thickness was 0.01 mm. Similarly, the cross-linked membrane CS/AA was prepared by dissolving 1.5 g (8.8 mmol) chitosan and 0.64 g (4.4 mmol) adipic acid in 100 mL

of distilled water, casting and heating the membrane at 100 °C under vacuum (0.9 bar) for 120 min. The membrane was placed in a desiccator to cool to room temperature after being washed with ethanol to remove residual adipic acid. Then, the degree of cross-linking (CLD%) was calculated according to the following equation (1) [37]:

$$\text{CLD}\% = k \times \frac{m_0 - m_t}{m_t} \times 100 \quad (1)$$

where  $m_0$  is the weight of the dried membrane before cross-linking,  $m_t$  is the weight of the dried membrane after cross-linking,  $k$  is a constant ( $=7.7698$ ) related to the reactants (chitosan/adipic acid).

### 2.3. Characterization of membranes

#### 2.3.1. Fourier transform infrared spectroscopy (FTIR)

FTIR spectra of the membranes after grinding were recorded using Nicolet 6700 in the range of 400–4000  $\text{cm}^{-1}$ , and 64 scans per spectra were recorded at a resolution of 2  $\text{cm}^{-1}$ . The samples for FTIR analysis were prepared by the KBr pellet method.

#### 2.3.2. Thermal properties of the membranes

Differential scanning calorimetry (DSC) for membranes were performed using a DSC131 DSC from (SETARAM). The scanning was performed using 10 mg of sample in a temperature range between 25 and 450 °C at a heating rate of 10 °C/min under nitrogen gas flow of 100 mL/min. Thermogravimetric analysis (TGA) for membranes were performed using a TG 50 from (Mettler Toledo). The scanning was performed using 10 mg of sample in a temperature range between 25 and 800 °C at a heating rate of 10 °C/min under nitrogen gas flow of 100 mL/min.

#### 2.3.3. Physical and surface properties

The porosity ( $\mathcal{E}\%$ ) of both membranes (CS, CS/AA) was determined based on the water uptake capacity. The membrane was soaked in distilled water for 24 h. Then, the porosity was calculated as shown in equation (2) [38]:

$$\mathcal{E}\% = \frac{(w_2 - w_1)}{(\rho_{\text{water}} \times s \times h)} \times 100 \quad (2)$$

where  $w_1$ : the dry membrane weight (g),  $w_2$ : the swollen membrane weight (g),  $\rho_{\text{water}}$ : water density ( $\text{g}/\text{cm}^3$ ),  $s$ : membrane surface area ( $1 \times 1$ )  $\text{cm}^2$ ,  $h$ : membrane thickness (cm).

The swelling degree (DS%) was calculated using equation (3) [39]:

$$\text{DS}\% = \frac{(w_2 - w_1)}{w_1} \times 100 \quad (3)$$

where  $w_1$ : the dry membrane weight (g) and  $w_2$ : the swollen membrane weight (g).

The hydrophobicity properties were determined by n-Hexane absorbency. The formula is shown in equation (4) [40]:

$$W_H\% = \frac{(w_2 - w_1)}{w_1} \times 100 \quad (4)$$

where  $w_1$ : the dry membrane weight (g) and  $w_2$ : the membrane weight after uptake n-Hexane (g).

The pure water permeability ( $Q_{\text{pw}}$ ) test was performed with a dead-end filtration system using distilled water and the pure water permeability was calculated using equation (5) [41]:

$$Q_{\text{pw}} = \frac{V}{S \times t} \quad (5)$$

where  $V$ : the permeate volume (l),  $s$ : the effective area of membrane ( $\text{m}^2$ ),  $t$ : represents time (h).

The average pore radius ( $r_p$ ) of the membranes was examined based on the filtration rate method and calculated using the Guerout–Elford–Ferry (GEF) formula expressed in equation (6) [42]:

$$r_p = \sqrt{\frac{(2.9 - 1.75 \times \mathcal{E}) \times 8 \times \eta \times h \times Q_{\text{pw}}}{\mathcal{E} \times S \times p}} \quad (6)$$

where  $\mathcal{E}$ : porosity of membrane (%),  $\eta$ : viscosity of water ( $8.9 \times 10^{-4}$  Pa·s),  $h$ : the thickness of membrane (m),  $Q_{\text{pw}}$ : the volume of permeate water per unit time ( $\text{m}^3/\text{s}$ ),  $s$ : the effective area of membrane ( $\text{m}^2$ ),  $p$ : the operating pressure (Pa).

The burst test of the membrane was carried out by a device which was developed in our laboratory. The membrane was placed on a 133.69  $\text{mm}^2$  ring, then pressurized water was applied to the membrane and the hydrostatic pressure was measured using a pressure regulator. The hydrostatic pressure was gradually increased and when the membrane ruptured the pressure dropped rapidly. The maximum pressure value was recorded as the burst pressure of the membrane [43]. Specific surface area and the distribution of average pore radius for CS/AA membrane was determined from  $\text{N}_2$  adsorption isotherm obtained at  $-196.15$  °C (Tri-Star II 3020).

CS/AA membrane was first degassed at 120 °C for 2 h before analysis. The Brunauer–Emmett–Teller (BET) equation was applied to  $N_2$  adsorption data for  $P/P_0$  between 0.3 and 0.6. The point of zero charge ( $pH_{pzc}$ ) of CS/AA was measured using the method as previously described [44], with some modification. NaCl (0.1 M) solutions at different pH were prepared. The initial pH of the solutions ( $pH_{initial}$ ) was adjusted at (4–11) using 0.1 M of HCl or NaOH aqueous solution. After that, 10 mg of membrane was added to 10 mL of different  $pH_{initial}$  solution, and the samples were shaken for 24 h at room temperature using SCI-O180-PRO LCD digital orbital shaker from (SCIOGEX). After 24 h, the final pH ( $pH_{final}$ ) was measured using a Martini pH meter (Mi-180 model). The  $pH_{pzc}$  value was determined from a plot of  $\Delta pH$  ( $pH_{final} - pH_{initial}$ ) versus  $pH_{initial}$ . The surface imaging was also performed using atomic force microscope (AFM) (Easy scan 2 flex AFM, Micro 40). The membrane area for the AFM measurement was  $(3 \times 3) \text{ cm}^2$ . The average roughness ( $S_a$ ) and the root mean square average of height deviation ( $S_q$ ) were calculated to evaluate the membrane's surface roughness.

#### 2.3.4. Stability of the membranes

Acidic chitosan membranes (CS, CS/AA) (which were not immersed in an alkaline solution or ethanol) were cut into square shapes, weighed ( $w_1$ ), immersed in distilled water, and incubated at room temperature for 24 h. Next, the samples were dried at 70 °C overnight and weighed again ( $w_2$ ). The weight loss ( $W_s\%$ ) was calculated using equation (7) [28]:

$$W_s\% = \frac{(w_1 - w_2)}{w_1} \times 100 \quad (7)$$

where  $w_1$ : the membrane weight before immersion (g) and  $w_2$ : the membrane weight after immersion (g).

The stability of the CS/AA membrane (immersed in ethanol to remove unreacted acid) at different pH (2.75, 3.17, 4.04, 5.41, 10.64, 11.07, 13.1) was studied following the same previous procedure.

#### 2.4. Ultrafiltration performance of CS/AA membrane

Water permeability and removal of both reactive yellow-145 (RY-145, 100 mg/L, 1.5 bar) and methylene blue (MB, 4.8 mg/L, 1 bar) at  $pH = 7.5$  for CS/AA were measured through a dead-end filtration system. Fig. 1 shows a schematic representation of the module and setup for testing the water permeation. The initial volume of the aqueous phase was 10 mL and the effective surface area of the membrane was  $118.7 \text{ mm}^2$ . The operating pressure was adjusted by introducing  $N_2$  gas at 25 °C. A magnetic stirrer was mounted near the membrane surface and stirred at a constant speed of 250 rpm in the aqueous phase, and the volume of permeated water was measured. Then, the volumetric water flux  $Q_{tw}(\text{L}/\text{m}^2 \cdot \text{h})$  and R% removal were then calculated using equations (8) and (9) [32]:

$$Q_{tw} = \frac{V}{S \cdot t} \quad (8)$$

$$R\% = \left(1 - \frac{C_p}{C_f}\right) \times 100 \quad (9)$$

where  $Q_{tw}$  represents flux for treated water ( $\text{L}/\text{m}^2 \cdot \text{h}$ ),  $V$  is the permeate volume (L),  $t$  represents time (h), and  $A$  is the effective area of membrane ( $\text{m}^2$ ),  $C_f$  the concentration of the feed solution (mg/L),  $C_p$  the concentration of the permeate (mg/L).

After the completion of the separation process, the dead-end filtration cell was emptied and a new solution of MB with a

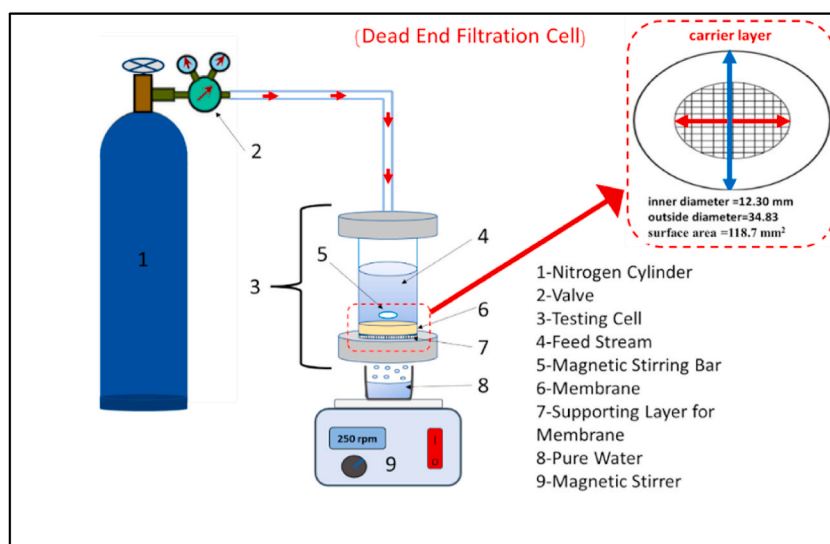


Fig. 1. Dead-End Filtration system.

concentration of 8 mg/L was added. The procedure was repeated five times with the same membrane. Subsequently, the volumetric water flux  $Q_{tw}(L/m^2.h)$  and R% removal of MB were calculated [45].

### 3. Results and discussion

#### 3.1. Structural analysis of membranes

FTIR was used to investigate changes in the chemical structure of chitosan membrane before and after cross-linking using AA. FTIR spectra of both CS and CS/AA membranes are shown in Fig. 2.

The FTIR spectra were consistent with the results of Cai M. et al. The amide I band for CS/AA membrane became weaker and narrower compared to that of CS membrane. In addition, new absorption shoulders at  $1558.2$  and  $1708.6$   $cm^{-1}$  attributed to the amide II and free carboxylic groups respectively were observed. The appearance of the absorption shoulder of the amide II suggests the formation of the amide bond [37]. The broad band at  $3450$   $cm^{-1}$ , which was assigned to the stretching of the hydroxyl groups  $-OH$ , was clearly overlapped with  $-N-H$  stretching, and was present in both spectra without any change [28]. Based on the FTIR spectra, a proposed formula for the membrane can be represented as shown in Fig. 3.

#### 3.2. Thermal properties

To investigate the pyrolysis behavior of CS and CS/AA membranes, TGA/DTG and DSC were carried out by heating the sample in dynamic nitrogen atmosphere. Fig. 4 shows the results of DSC analysis of the chitosan membranes before and after cross-linking with adipic acid.

The thermogram of CS shows an endothermic peak at  $95.14$   $^{\circ}C$  with a value of  $\Delta H = 265.5$  J/g, while the endothermic peak for CS/AA was observed at  $107.54$   $^{\circ}C$  with a value of  $\Delta H = 209.7$  J/g. This indicates an increase in the hydrophobic properties of the membrane after cross-linking which agree with the results shown in Table .1 and consistent with other studies presented [46,47]. The glass transition temperature  $T_g$  of the cross-linked polymer was determined to be  $57.04$   $^{\circ}C$ , while it was not observed in the thermogram of pure chitosan. This indicates an improvement in the flexibility of the membrane due to the introduction of adipic acid into the structure, which leads to a decrease in the degree of crystallinity of the cross-linked membrane [37]. In addition, each membrane had a different melting point  $T_m$ . The  $T_m$  of the CS membrane is  $145.6$   $^{\circ}C$ , while the  $T_m$  for CS/AA membrane increased and reached  $159.02$   $^{\circ}C$  [30]. The exothermic peak is related to the complete degradation of the polymer. Pure chitosan membrane shows one exothermic peak at  $301.5$   $^{\circ}C$ . In the case of CS/AA the exothermic decomposition peak shifts to  $268.58$   $^{\circ}C$ . It indicates that the addition of adipic acid reduces the thermal stability of membrane. This result is consistent with [48]. When discussing the enthalpy values for both membranes, we find that: the enthalpy of degradation for CS membrane was  $\Delta H = -342.2$  J/g, while the CS/AA membrane is  $\Delta H = -208.9$  J/g. So that might be the reason for the decrease of  $\Delta H$  value after cross-linking is due to the formation of the amide bond, whose degradation was an endothermic process and thus the intensity of the exothermic peak decreases, especially since the CLD% value was about 35 %. On the other hand, Fig. 5 (a) and (b) show the results of TGA and DTG analysis respectively of the chitosan membranes before and after cross-linking with adipic acid.

There were three characteristic temperature intervals of weight loss. The first weight loss corresponding to the loss of moisture for two membranes. The CS membrane begins non-oxidative thermal decomposition in a nitrogen atmosphere at  $240$   $^{\circ}C$ , while the CS/AA membrane begins decomposing at  $185.8$   $^{\circ}C$ . The reason for the weight decrease is due to the depolymerization of chitosan chains through cleavage of glycosidic bonds and dissociation of the new amide bonds in the membrane structure [49]. The cross-linking process decreased the polymer's thermal stability because the interaction between adipic acids and chitosan's amino groups can destroy the chitosan's crystalline structure [50]. The third weight loss corresponding to decomposition of the resulting dissociation

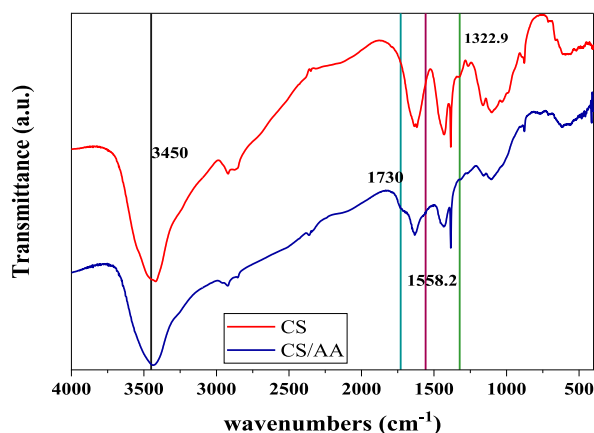


Fig. 2. FTIR spectrum before and after cross-linking reaction.

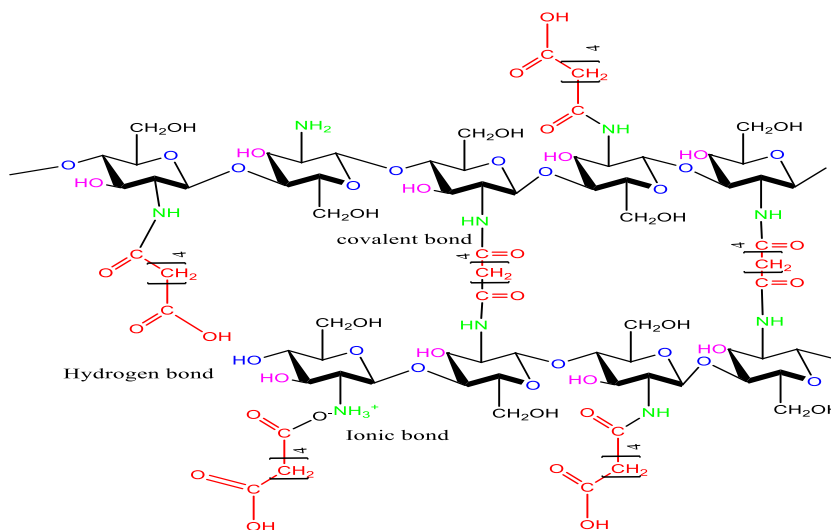


Fig. 3. Schematic representation of the possible interaction between chitosan and adipic acid.

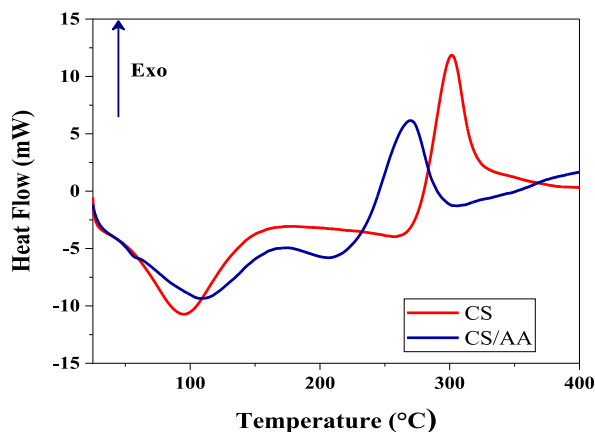


Fig. 4. DSC curves for CS and CS/AA.

**Table 1**  
Membranes properties (CS, CS/AA).

Type of membrane	CS	CS/AA
$D_s\%$	$121.88 \pm 0.03$	$96.39 \pm 0.05$
$\xi\%$	$36.55 \pm 0.72$	$73.95 \pm 0.75$
$r_p$ (nm)	$7.41 \pm 0.41$	$1.93 \pm 0.05$
$P_b$ (kPa)	$54.00 \pm 2$	$149.67 \pm 0.58$
CLD%	–	$35.48 \pm 0.68$
$Q_{pw}$ ( $\frac{L}{m^2h}$ )	$4.502 \pm 0.397$	$1.237 \pm 0.055$
$W_H\%$	$12.34 \pm 0.05$	$37.82 \pm 0.13$

products from both membranes.

### 3.3. Physical and surface properties of membranes

Table .1 shows the properties of both CS and CS/AA membranes. It was observed after the cross-linking reaction that the  $D_s\%$  decreased with the improvement of hydrophobic properties, which was related to an increase in the  $W_H\%$ , due to the formation of new amide bonds. In addition, the  $\xi\%$  increased due to the presence of adipic acid between the polymer chains, with a lower  $r_p$  value compared to that of the CS membrane. This explained the lower flux of pure water through the CS/AA membrane. On the other hand,

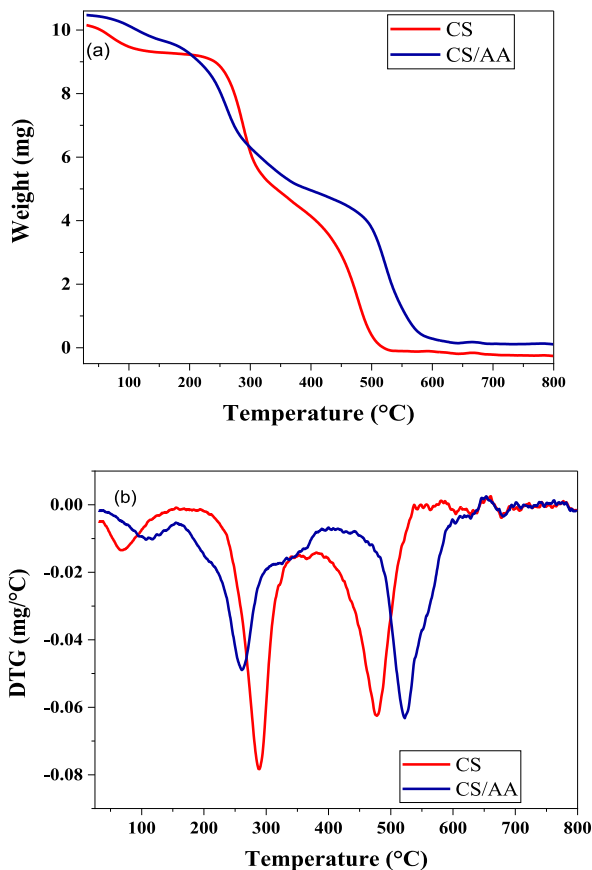


Fig. 5. TGA (a) and DTG (b) thermogram for (CS, CS/AA).

the cross-linking increased the burst pressure of the CS/AA membrane, which enabled the membrane to withstand high pressure.

It should be noted that the degree of swelling could be improved by introducing nanofillers [51] or hydrophilic polymer [32] into the CS/AA matrix during the membrane syntheses process which, increase the flux value.

The specific surface area, total pore volume, and the average pore radius distribution were determined and the results obtained are shown in Fig. 6 and Fig. 7.

The CS/AA membrane had a relatively low effective specific surface area about 1.8 m<sup>2</sup>/g, and the values of the pore radius were

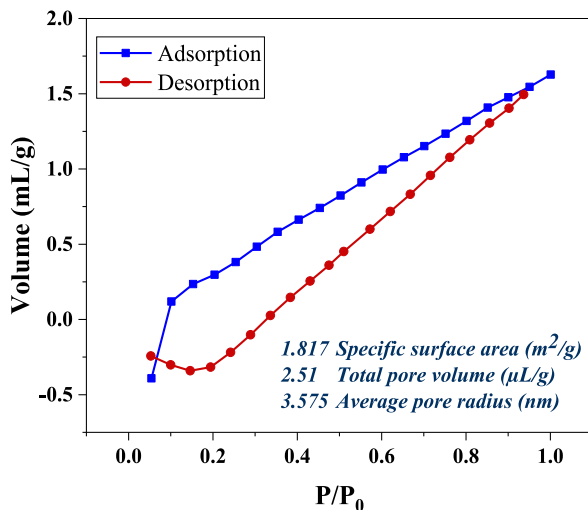


Fig. 6. BET analysis of nitrogen adsorption-desorption isotherm for CS/AA membrane.

clearly close to those obtained by the (GEF) method (see Table 1.). In addition, the distribution of average pore radius was in the range from 2 to 27 nm, so the CS/AA membrane was classified into the ultrafiltration membranes [52]. Fig. 8 shows the surface charge of the CS/AA membrane at variable pH values.

The CS/AA membrane had a zero-charge point at pH = 7.8, and at pH < 7.8, the membrane had a positive charge due to the amine groups protonated, and at pH > 7.8, the membrane had a negative charge due to the removal of protons from the carboxyl or hydroxyl groups.

AFM was used to analyze the changes in the surface morphology of chitosan membrane before and after cross-linking. The average surface roughness ( $S_q$ ), and the mean value of the surface roughness coefficient ( $S_a$ ) were calculated to evaluate the effect of AA on the membrane surface roughness.

As shown in Fig. 9, we notice an increase in the average surface roughness of 56.49 nm after cross-linking. This is consistent with Olewnik-Kruszkowska, E et al. [53]. It should be noted that increasing the surface roughness would reduce the permeate fluxes due to the accumulation and adhesion of pollutant particles on the membrane surface [54].

Fig. 10 shows the results of the effect of distilled water on the weight loss of ionic CS and CS/AA membranes.

There was a clear significant difference in  $W_s\%$  values for both membranes, which was attributed to the release of acid from the membrane to the aqueous phase, with the collapse of the membrane structure. Therefore, the cross-linked membrane showed better capability of water resistance, compared to the pure membrane [26]. Fig. 11 shows the effect of pH change on the weight loss of CS/AA membrane.

The CS/AA membrane had high resistance to both acid and alkaline phases, but significant weight losses were observed at pH below 2.75 or above 11.08. The cross-linking process links the polymer chains together, and reduces the number of protonated amine groups available to induce membrane dissolution. Hence, the membrane is able to work in acidic and alkaline environments to separate pollutants from aqueous phase. This is consistent with Rezik, S B. et al. [55]. It was observed that using sodium tripolyphosphate (STPP) as a cross-linking agent increases the stability of the membrane in aqueous media at pH (2, 4, 6.2, 9) compared to pure chitosan membrane.

## 4. Separation performance of CS/AA membrane

### 4.1. Determination of RY-145 removal and water flux

Table 2 shows the dye removal and flux values for RY-145 at an initial concentration of 100 mg/L and pH of 7.5.

The removal efficiency of RY-145 and  $Q_{tw}$  increased with an increase in the pressure applied to the CS/AA membrane, due to the increase in the compaction of the membrane [56]. This hinders the passage of the dye particles through the nanopores according to the size exclusion mechanism due to the large molecular weight of the dye, while water molecules can pass through the nanopores [57]. In addition, the adsorption function of the dye on the surface of CS/AA by association with the effective functional groups. In particular, CS/AA had a positive charge at pH = 7.5 (see Fig. 8.) and RY-145 molecules had a negative charge, so there was an electrostatic attraction between the membrane and the dye molecules. Fig. 12 shows the color change of the membrane before and after the separation process as a result of the affinity of RY-145 dye to the CS/AA membrane.

The fouling phenomenon for membrane is not desirable because, it affects the membrane separation performance. By reviewing the literature data, there are many solutions to reduce this issue. For example, controlling the surface charge of the membrane by changing pH of the medium that may cause the repulsion or affinity of the particles towards the membrane [58], according to Fig. 13.

Fig. 14 shows the spectral scanning between (400–800) nm for RY-145, and the color change of dye solution before and after the

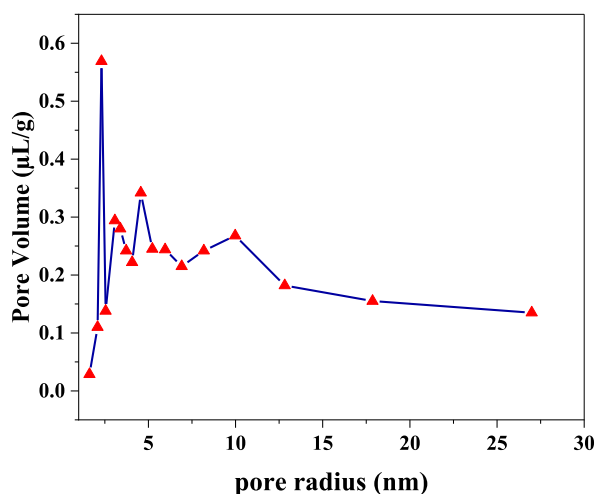


Fig. 7. The average pore radius distribution for CS/AA membrane.

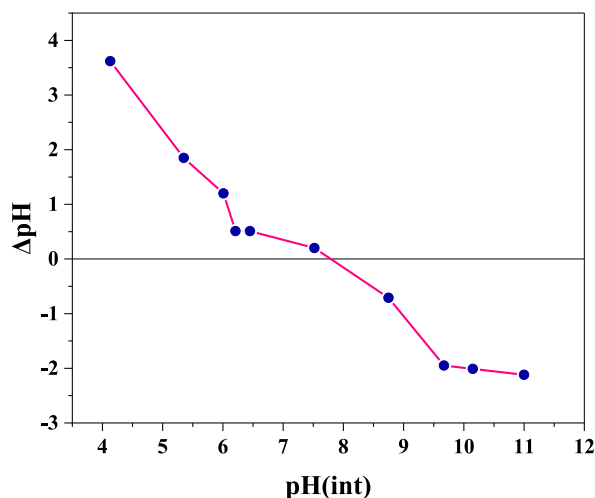


Fig. 8. Surface charge of the CS/AA membrane at variable pH values.

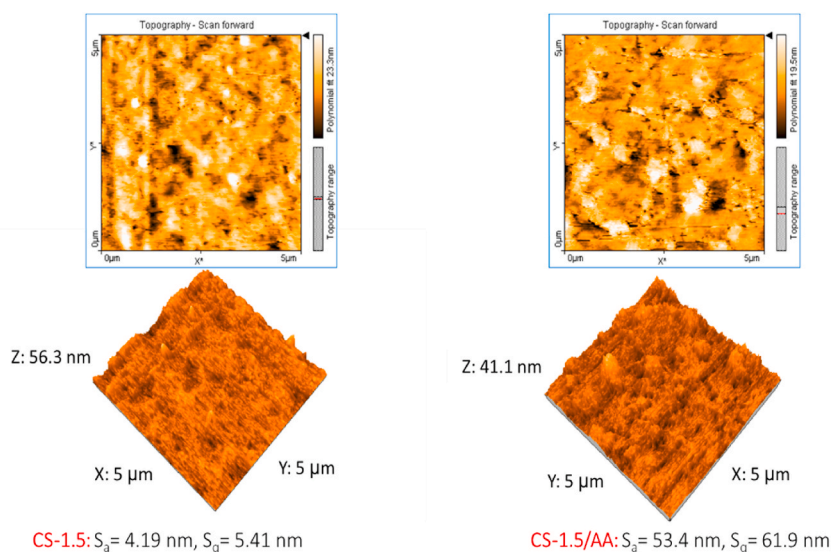


Fig. 9. The 2D and 3D AFM images of CS and CA-1.5/AA membranes.

separation process.

#### 4.2. Determination of MB removal and water flux

Table 3 shows the removal and flux values for MB at two initial concentrations of 4 and 8 mg/L at pH of 7.5 applying a pressure of 1 bar.

The CS/AA membrane was able to completely remove MB dye from the aqueous phase at the studied concentrations with similar flux value of about  $1 \text{ (L/m}^2\text{.h)}$ . But it is obviously noted that the  $Q_{tw}$  of membrane CS/AA under dye solution is slightly lower than  $Q_{pw}$  at the same conditions due to the greater osmotic pressure of dyes solutions compared to distilled water, as well as owing to the membrane pores blocked by dye molecules according to Fig. 12 [59].

Fig. 15 shows the spectral scanning between (400–800) nm for MB, and the color change of dye solution before and after the separation process.

#### 4.3. Effect of continuous separations of MB using CS/AA

Table 4 shows the results of repeated separation of MB: 8 mg/L during five continuous separation stages using a single layer of membrane CS/AA with a pressure of 1 bar.

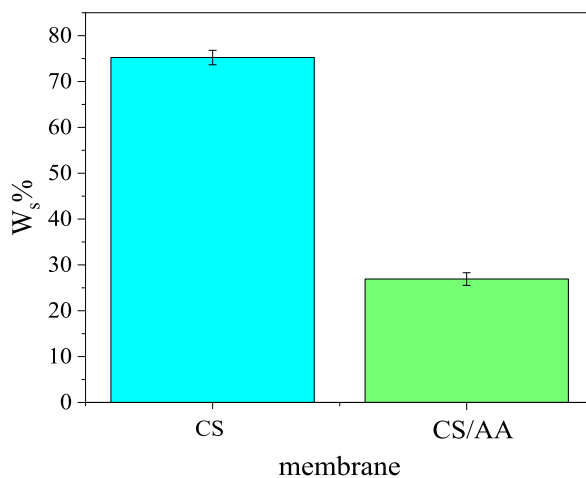


Fig. 10. Weight loss in ionic chitosan membranes before and after cross-linking.

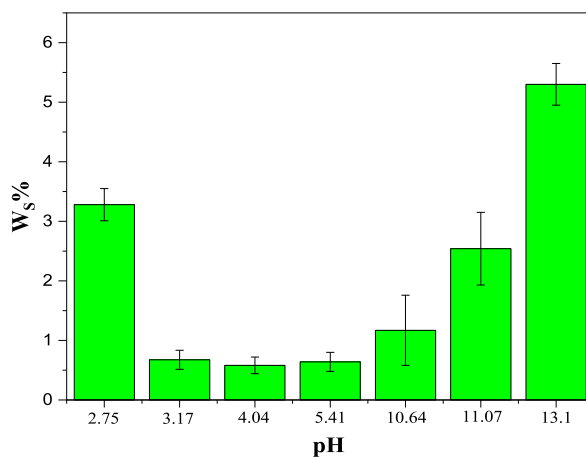


Fig. 11. Weight loss in CS/AA membrane at different pH values.

**Table 2**  
Removal% and flux for RY-145 solution using CS/AA.

$Q_{tw}$ (L/m <sup>2</sup> .h)	Removal (%)	Pressure (bar)
1.066 ± 0.026	94.21 ± 0.28	1
2.09 ± 0.098	96.27 ± 0.70	1.5



Fig. 12. The photograph of the CS/AA membrane before and after the RY-145 separation process.

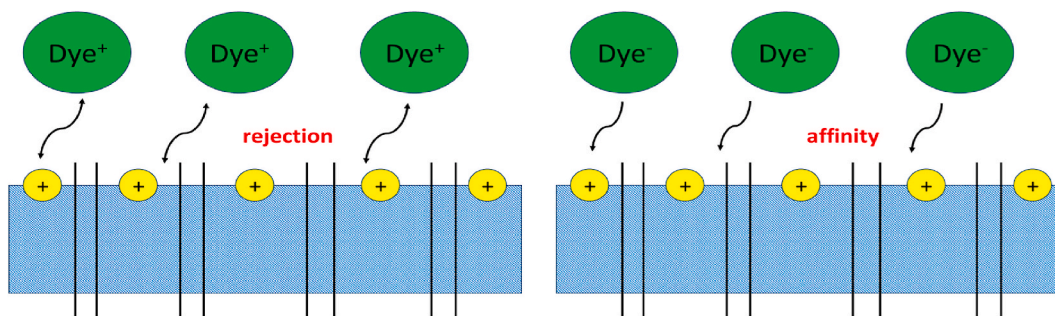


Fig. 13. The effect of surface charge of membrane on repulsion or affinity of the dye.

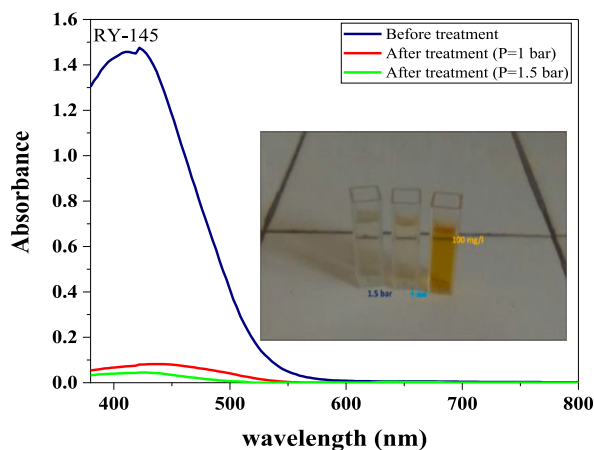


Fig. 14. spectrum scanning of RY-145 dye before and after treatment.

**Table 3**  
Removal% and flux for MB solution using CS/AA.

$Q_{rw}$ (L/m <sup>2</sup> .h)	Removal (%)	concentration (mg/L)
1.010 ± 0.074	100 ± 0.0	4
0.936 ± 0.144	100 ± 0.0	8

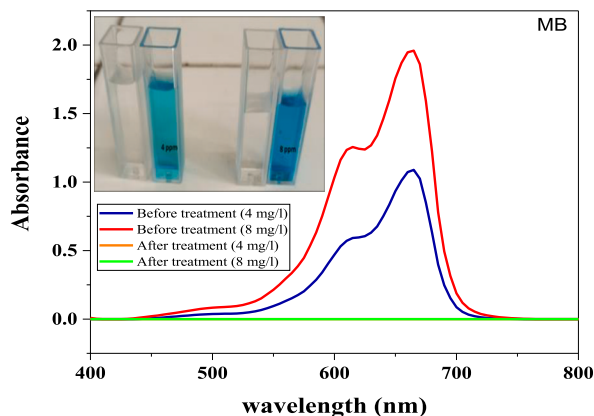


Fig. 15. spectrum scanning of MB dye before and after treatment.

The membrane efficiency CS/AA remained constant without being affected by the continuous separation processes. Donnan exclusion plays an important role in the rejecting of MB [60], especially at pH = 7.5, the surface charge of the membrane is positive (see Fig. 8.), and the dye MB is a basic dye that had a positive charge in the phase, therefore electrostatic repulsion will occur between the membrane and the dye. In addition, the large molecular weight plays an important role in preventing the dye from passing through the membrane nanopores.

Fig. 16 shows a photograph of the CS/AA membrane before and after MB separation during five separation stages without color change to the membrane surface, meaning that adsorption did not play a significant role in the separation process, especially the specific surface area was small (see Fig. 6).

Table .5 shows the removal efficiency and flux values at different working conditions for the CS/AA membrane compared with other literature.

## 5. Conclusions

The ultrafiltration membrane based on chitosan/adipic acid CS/AA was prepared by binding the polymer chains with new amide bonds for separation the organic dyes from aqueous phase. The cross-linking process made the membrane highly resistant to acidic and alkaline phases, with increase the burst pressure, porosity, surface roughness, and flexibility. The cross-linking process increased the hydrophobic properties of the membrane and consequently the permeation flux decreased. In contrast, CS/AA membrane achieved high efficiency in removing MB and RY-145 from the aqueous phase due to due to nanopores and surface charge, and it can be used up to five cycles of separation without losing its effectiveness. The results affirmed that the CS/AA cross-linked membrane is very suitable to separate organic dyes from the aqueous phase with high efficiency.

## Statistical analysis

All data was displayed as the mean  $\pm$  SD, n = 3, SD: Standard deviation.

## Funding statement

This research did not receive any specific grant from funding agencies in the public, commercial, or not-for-profit sectors.

## Additional information

No additional information is available for this paper.

## Data availability statement

Data included in article/supp. material/referenced in article.

## CRedit authorship contribution statement

**Khaled Hab Alrman:** Writing – review & editing, Writing – original draft, Validation, Software, Resources, Project administration, Methodology, Investigation, Formal analysis, Data curation. **Sahar Alhariri:** Writing – review & editing, Writing – original draft, Validation, Supervision, Software, Data curation, Conceptualization. **Iman Al- Bakri:** Writing – review & editing, Writing – original draft, Validation, Methodology.

## Declaration of competing interest

The authors declare that they have no known competing financial interests or personal relationships that could have appeared to influence the work reported in this paper.

**Table 4**

Continuous separation of MB: 8 mg/L using CS/AA membrane at pH (7.5) and P (1) bar.

$Q_{tw}$ (L/m <sup>2</sup> .h)	Removal (%)	concentration(mg/L)	Feed solution
0.994 $\pm$ 0.135	100 $\pm$ 0.0	8	1
1.013 $\pm$ 0.120	100 $\pm$ 0.0	8	2
1.053 $\pm$ 0.082	100 $\pm$ 0.0	8	3
1.012 $\pm$ 0.065	100 $\pm$ 0.0	8	4
1.013 $\pm$ 0.064	100 $\pm$ 0.0	8	5

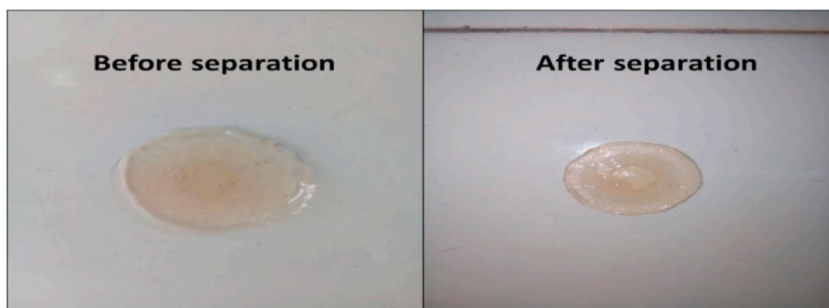


Fig. 16. The photograph of the CS/AA membrane before and after the MB separation process.

Table 5

Comparison of Removal% and Flux (L/m<sup>2</sup>.h) of Cs/AA membrane with other literature.

Membrane	Conditions	Removal%	Flux (L/m <sup>2</sup> .h)	Reference
CS/AA	RY-145 (100) mg/L, p= (1,1.5) bar, pH = 7.5	94, 96	1.066, 2.09	This work
PVDF/BNT (1–5) %	RY-145 (1000) mg/L, p = 2 bar	86–94	15–17	[61]
TiO <sub>2</sub> /ZnAl <sub>2</sub> O <sub>4</sub>	RY-145 (40) mg/L, p = 8 bar, pH= (3–9)	100	25–40	[62]
CS/AA	MB (4,8) mg/L, P = 1 bar, pH = 7.5	100	0.936, 1	This work
CA/NAC	MB (10) mg/L	80	–	[63]
Psf-GO (1–4) %	MB (40–150) mg/L, p (2–8) bar, pH (3-13)	80–100	75	[64]

## Acknowledgment

The authors would like to thank Damascus University and Atomic Energy Commission of Syria for providing the supplies to carry out this work and dr. Ibrahim Alghoraibi for his fruitful help.

## References

- [1] Q. Long, Z. Zhang, G. Qi, Z. Wang, Y. Chen, Z.Q. Liu, Fabrication of chitosan nanofiltration membranes by the film casting strategy for effective removal of dyes/salts in textile wastewater, *ACS Sustain. Chem. Eng.* 8 (6) (2020) 2512–2522.
- [2] J. Xiao, W. Lv, Z. Xie, Y. Tan, Y. Song, Q. Zheng, Environmentally friendly reduced graphene oxide as a broad-spectrum adsorbent for anionic and cationic dyes via  $\pi$ - $\pi$  interactions, *J. Mater. Chem. A* 4 (31) (2016), 12126–1213.
- [3] L.D. Ardila-Leal, R.A. Poutou-Piñales, A.M. Pedroza-Rodríguez, B.E. Quevedo-Hidalgo, A brief history of colour, the environmental impact of synthetic dyes and removal by using laccases, *Molecules* 26 (13) (2021) 3813.
- [4] B. Lellis, C.Z. Fávoro-Polonio, J.A. Pamphile, J.C. Polonio, Effects of textile dyes on health and the environment and bioremediation potential of living organisms, *BIORI* 3 (2) (2019) 275–290.
- [5] Arcadio P. Sincero, Gregoria A. Sincero, *Physical-chemical Treatment of Water and Wastewater*, CRC press, 2002.
- [6] Kingsley Tamunokuro Amakiri, Anyela Ramirez Canon, Marco Molinari, Athanasios Angelis-Dimakis, Review of oilfield produced water treatment technologies, *Chemosphere* 298 (2022) 134064.
- [7] E. Obotey Ezugbe, S. Rathilal, Membrane technologies in wastewater treatment: a review, *Membranes* 10 (5) (2020) 89.
- [8] R. Castro-Muñoz, A critical review on electrospun membranes containing 2D materials for seawater desalination, *Desalination* 555 (2023) 116528.
- [9] J.R.A. Cosme, R. Castro-Muñoz, V. Vatanpour, Recent advances in nanocomposite membranes for organic compound remediation from potable waters, *ChemBioEng Rev.* 10 (2) (2023) 112–132.
- [10] N.H. Othman, N.H. Alias, N.S. Fuzil, F. Marpani, M.Z. Shahrudin, C.M. Chew, A.F. Ismail, A review on the use of membrane technology systems in developing countries, *Membranes* 12 (1) (2021) 30.
- [11] R. Castro-Munoz, K.V. Agrawal, Z. Lai, J. Coronas, Towards large-scale application of nanoporous materials in membranes for separation of energy-relevant gas mixtures, *Separ. Purif. Technol.* 308 (2023) 122919.
- [12] R. Castro-Muñoz, M.Z. Ahmad, M. Malankowska, J. Coronas, A new relevant membrane application: CO<sub>2</sub> direct air capture (DAC), *Chem. Eng. J.* 446 (2022) 137047.
- [13] W. Jankowski, G. Li, W. Kujawski, J. Kujawa, Recent development of membranes modified with natural compounds: preparation methods and applications in water treatment, *Separ. Purif. Technol.* 302 (2022) 122101.
- [14] X. Shi, G. Tal, N.P. Hankins, V. Gitis, Fouling and cleaning of ultrafiltration membranes: a review, *J. Water Proc. Eng.* 1 (2014) 121–138.
- [15] X. Li, L. Jiang, H. Li, Application of ultrafiltration technology in water treatment, in: *IOPConference Series: Earth and Environmental Science*, vol. 186, IOP Publishing, 2018, October 012009.
- [16] S.R. Mousavi, M. Asghari, N.M. Mahmoodi, Chitosan-wrapped multiwalled carbon nanotube as filler within PEBA thin film nanocomposite (TFN) membrane to improve dye removal, *Carbohydrate Polym.* 237 (2020) 116128.
- [17] Sabu Thomas, Anitha Pius, Sreerag Gopi (Eds.), *Handbook of Chitin and Chitosan: Volume 2: Composites and Nanocomposites from Chitin and Chitosan, Manufacturing and Characterisations*, Elsevier, 2020.
- [18] Preeti Pal, Anjali Pal, Kazunori Nakashima, Brijesh Kumar Yadav, Applications of chitosan in environmental remediation: a review, *Chemosphere* 266 (2021) 128934.
- [19] Yuzhe Zhang, Meiwen Zhao, Qian Cheng, Chao Wang, Hongjian Li, Xiaogang Han, Zhenhao Fan, Gaoyuan Su, Deng Pan, Zhongyu Li, Research progress of adsorption and removal of heavy metals by chitosan and its derivatives: a review, *Chemosphere* 279 (2021).
- [20] Angela Spoială, Cornelia-Ioana Ilie, Denisa Ficai, Anton Ficai, Ecaterina Andronescu, Chitosan-based nanocomposite polymeric membranes for water purification—a review, *Materials* 14 (9) (2021) 2091.
- [21] Petronela Nechita, Applications of chitosan in wastewater treatment, Biological activities and application of marine polysaccharides 1 (2017) 209–228.

- [22] R. Yahya, R.F. Elshaarawy, Highly sulfonated chitosan-polyethersulfone mixed matrix membrane as an effective catalytic reactor for esterification of acetic acid, *Catal. Commun.* 173 (2023) 106557.
- [23] S. Jana, S. Jana (Eds.), *Functional Chitosan: Drug Delivery and Biomedical Applications*, Springer Nature, 2020.
- [24] O.U. Akakuru, H. Louis, P.I. Amos, O.C. Akakuru, E.I. Nosike, E.F. Ogulewe, The chemistry of chitin and chitosan justifying their nanomedical utilities, *Biochem. Pharmacol.* 7 (241) (2018), 2167-0501.
- [25] F. Wu, Y. Qi, X. Wang, Y. Shen, H. Li, Study on the preparation of hydroxypropyl C/hitosan and its optimal reaction conditions, *Chemistry Journal* 5 (2020).
- [26] F. Gilbertson, Improving Wet Performance of Chitosan-Xylan Bioplastic Using a Biobased Additive, 2017.
- [27] V.D.A. Sangkota, R.A. Lusiana, Y. Astuti, Blend membrane of succinic acid-crosslinked chitosan grafted with heparin/PVA-PEG (polyvinyl alcohol-polyethylene glycol) and its characterization, in: *IOP Conference Series: Mater. Sci. Eng.*, vol. 349, IOP Publishing, 2018 012065, 1.
- [28] B. Moghadas, A. Solouk, D. Sadeghi, Development of chitosan membrane using non-toxic crosslinkers for potential wound dressing applications, *Polym. Bull.* 78 (2021) 4919–4929.
- [29] A. Ghosh, M.A. Ali, Studies on physicochemical characteristics of chitosan derivatives with dicarboxylic acids, *J. Mater. Sci.* 47 (2012) 1196–1204.
- [30] S.T. Sam, Effect of adipic acid as crosslinker on the tensile and thermal properties of rice straw cellulose nanocrystals/chitosan nanocomposites, *Malaysian J. Microsc.* 16 (2020) 1.
- [31] P.H. Chen, T.Y. Kuo, F.H. Liu, Y.H. Hwang, M.H. Ho, D.M. Wang, H.J. Hsieh, Use of dicarboxylic acids to improve and diversify the material properties of porous chitosan membranes, *J. Agric. Food Chem.* 56 (19) (2008) 9015–9902.
- [32] A. Raza, A. Kayani, A. Sabir, A. Ahmad, T. Hussain, M.H. Raza, R.U. Khan, Synthesis and investigation of desalinating, antibacterial, and mechanical properties of tetraethylorthosilicate crosslinked chitosan/polyethylene glycol (PEG-300) membranes for reverse osmosis, *J. Appl. Polym. Sci.* 137 (28) (2020) 48870.
- [33] I. Ali, M.A. Raza, R. Mehmood, A. Islam, A. Sabir, N. Gull, R.U. Khan, Novel maleic acid, crosslinked, nanofibrous chitosan/poly (vinylpyrrolidone) membranes for reverse osmosis desalination, *Int. J. Mol. Sci.* 21 (19) (2020) 7338.
- [34] A.H. Chen, S.C. Liu, C.Y. Chen, C.Y. Chen, Comparative adsorption of Cu (II), Zn (II), and Pb (II) ions in aqueous solution on the crosslinked chitosan with epichlorohydrin, *J. Hazard Mater.* 154 (1–3) (2008) 184–191.
- [35] J.M. Sosa, V.F. Medina, C.S. Griggs, V.G. Gude, Crosslinking Graphene Oxide and Chitosan to Form Scalable Water Treatment Membranes, Mississippi State University, 2017.
- [36] Ryo-ichi Nakayama, Koki Katsumata, Yuta Niwa, Norikazu Namiki, Dependence of waterpermeable chitosan membranes on chitosan molecular weight and alkali treatment, *Membranes* 10 (11) (2020) 351.
- [37] M. Cai, J. Gong, J. Cao, Y. Chen, X. Luo, In situ chemically crosslinked chitosan membrane by adipic acid, *J. Appl. Polym. Sci.* 128 (5) (2013) 3308–3314.
- [38] Z. Guo, R. Xiu, S. Lu, X. Xu, S. Yang, Y. Xiang, Submicro-pore containing poly (ether sulfones)/polyvinylpyrrolidone membranes for high-temperature fuel cell applications, *J. Mater. Chem. A* 3 (16) (2015) 8847–8854.
- [39] H.C.L. De Oliveira, J.L.C. Fonseca, M.R. Pereira, Chitosan-poly (acrylic acid) polyelectrolyte complex membranes: preparation, characterization and permeability studies, *Biomater. Sci., Polymer Edition* 19 (2) (2008) 143–160.
- [40] T.M. Tamer, B.Y. Eweida, A.M. Omer, H.M. Soliman, S.M. Ali, A.A. Zaatot, M.S. Mohy- Eldin, Removal of oil spills by novel amphiphilic Chitosan-g-Octanal Schiff base polymer developed by click grafting technique, *J. Saudi Chem. Soc.* 25 (12) (2021) 101369.
- [41] J.F. Li, Z.L. Xu, H. Yang, L.Y. Yu, M. Liu, Effect of TiO<sub>2</sub> nanoparticles on the surface morphology and performance of microporous PES membrane, *Appl. Surf. Sci.* 255 (9) (2009) 4725–4732.
- [42] F. Chen, X. Shi, X. Chen, W. Chen, An iron (II) phthalocyanine/poly (vinylidene fluoride) composite membrane with antifouling property and catalytic self-cleaning function for highefficiency oil/water separation, *J. Membr. Sci.* 552 (2018) 295–304.
- [43] K. Wang, A.A. Abdalla, M.A. Khaleel, N. Hilal, M.K. Khraisheh, Mechanical properties of water desalination and wastewater treatment membranes, *Desalination* 401 (2017) 190–205.
- [44] G.G. Celestino, R.R. Henriques, A.L. Shiguihara, V.R. Constantino, R. de Siqueira Melo, J. Amim Júnior, Adsorption of gallic acid on nanoclay modified with poly (diallyldimethylammonium chloride), *ESPR* 26 (2019) 28444–28454.
- [45] Y. Du, Y. Li, T. Wu, A superhydrophilic and underwater superoleophobic chitosan–TiO<sub>2</sub> composite membrane for fast oil-in-water emulsion separation, *RSC Adv.* 7 (66) (2017) 41838–41846.
- [46] S. Jana, A. Saikia, M.K. Purkait, K. Mohanty, Chitosan based ceramic ultrafiltration membrane: preparation, characterization and application to remove Hg (II) and as (III) using polymer enhanced ultrafiltration, *J. Chem. Eng.* 170 (1) (2011) 209–219.
- [47] D.R. Bhumkar, V.B. Pokharkar, Studies on effect of pH on cross-linking of chitosan with sodium tripolyphosphate: a technical note, *AAPS PharmSciTech* 7 (2006) E138–E143.
- [48] M. Pieróg, J. Ostrowska-Czubenko, M. Gierszewska-Drużyńska, Thermal degradation of double crosslinked hydrogel chitosan membranes, *Progress on Chemistry and Application of Chitin and its Derivatives* 17 (2012) 71–78.
- [49] D. de Britto, S.P. Campana-Filho, Kinetics of the thermal degradation of chitosan, *Thermochim. Acta* 465 (1–2) (2007) 73–82.
- [50] L. Zhuang, X. Zhi, B. Du, S. Yuan, Preparation of elastic and antibacterial chitosan–citric membranes with high oxygen barrier ability by in situ cross-linking, *ACS Omega* 5 (2) (2020) 1086–1097.
- [51] R. Castro-Munoz, Breakthroughs on tailoring vaporation membranes for water desalination: a review, *Water Res.* 187 (2020) 116428.
- [52] H. Alfannakh, H. Abdallah, S.S. Ibrahim, B. Souayeh, Low-pressure membrane for water treatment applications, *Int. J. Polym. Sci.* 1–7 (2020).
- [53] E. Olewnik-Kruszkowska, M. Gierszewska, S. Grabska-Zielińska, J. Skopińska-Wisniewska, E. Jakubowska, Examining the impact of squaric acid as a crosslinking agent on the properties of chitosan-based films, *Int. J. Mol. Sci.* 22 (7) (2021) 3329.
- [54] D. Lee, Y.J. Cha, Y. Baek, S.S. Choi, Y. Lee, Relationships among permeability, membrane roughness, and eukaryote inhabitation during submerged gravity-driven membrane (GDM) filtration, *Appl. Sci.* 10 (22) (2020) 8111.
- [55] S.B. Rezik, S. Gassara, J. Bouaziz, S. Baklouti, A. Deratani, Performance enhancement of kaolin/chitosan composite-based membranes by cross-linking with sodium tripolyphosphate: preparation and characterization, *Membranes* 13 (2) (2023) 229.
- [56] L. Wang, T. Cao, J.E. Dykstra, S. Porada, P.M. Biesheuvel, M. Elimelech, Salt and water transport in reverse osmosis membranes: beyond the solution-diffusion model, *ES&T* 55 (24) (2021) 16665–16675.
- [57] N.S. Suhailim, N. Kasim, E. Mahmoudi, I.J. Shamsudin, A.W. Mohammad, F. Mohamed Zuki, N.L.A. Jamari, Rejection mechanism of ionic solute removal by nanofiltration membranes: an overview, *Nanomaterials* 12 (3) (2022) 437.
- [58] D. Pichardo-Romero, Z.P. Garcia-Arce, A. Zavala-Ramírez, R. Castro-Munoz, Current advances in biofouling mitigation in membranes for water treatment: an overview, *Processes* 8 (2) (2020) 182.
- [59] S.M.M. Kabir, H. Mahmud, H. Schoenberger, Recovery of dyes and salts from highly concentrated (dye and salt) mixed water using nano-filtration ceramic membranes, *Heliyon* 8 (11) (2022) e11543.
- [60] B. Doménech, J. Bastos-Arrieta, A. Alonso, J. Macanás, M. Muñoz, D.N. Muraviev, Bifunctional polymer-metal nanocomposite ion exchange materials. *Ion Exchange Technologies*, 2012, pp. 35–72.
- [61] E. Pramono, R. Alfiansyah, M. Ahdiat, D. Wahyuningrum, C.L. Radiman, Hydrophilic poly (vinylidene fluoride)/bentonite hybrid membranes for microfiltration of dyes, *Mater. Res. Express* 6 (10) (2019) 105376.
- [62] H. Loukili, M. Persin, S.A. Younsi, A. Albizane, M. Bouhria, A. Larbot, Removal of textile dyes from waste water by ceramic ultrafiltration membrane, in: *Actes de Congrès Watmed 2 International Conference*, 2005, pp. 14–17. Novembre (2005).
- [63] O.A. Koriem, A.M. Kamel, W. Shaaban, M.F. Elkady, Enhancement of dye separation performance of eco-friendly cellulose acetate-based membranes, *Sustainability* 14 (22) (2022) 14665.
- [64] K. Sunil, P. Sherugar, S. Rao, C. Lavanya, G.R. Balakrishna, G. Arthanareeswaran, M. Padaki, Prolific approach for the removal of dyes by an effective interaction with polymer matrix using ultrafiltration membrane, *J. Environ. Chem. Eng.* 9 (6) (2021) 106328.